Environmental Science and Ecotechnology 18 (2024) 100327

Contents lists available at ScienceDirect

Environmental Science and Ecotechnology

journal homepage: www.journals.elsevier.com/environmental-science-and-ecotechnology/

Original Research

Sampling efficiency of a polyurethane foam air sampler: Effect of temperature

Qiu-Liang Cai [a, b], Cen-Yan Huang [c], Lei Tong [a, d], Ning Zhong [e], Xiao-Rong Dai [a, c], Jian-Rong Li [a, d], Jie Zheng [a, d], Meng-Meng He [a, d], Hang Xiao [a, *]

[a] Key Laboratory of Urban Environment and Health, Ningbo Observation and Research Station, Institute of Urban Environment, Chinese Academy of Sciences, Xiamen, 361021, China
[b] Key Laboratory of Ecological Environment Analysis and Pollution Control in Western Guangxi Region, College of Agriculture and Food Engineering, Baise University, Baise, 533000, China
[c] College of Biological and Environmental Sciences, Zhejiang Wanli University, Ningbo, 315100, China
[d] Zhejiang Key Laboratory of Urban Environmental Processes and Pollution Control, CAS Haixi Industrial Technology Innovation Center in Beilun, Ningbo, 315830, China
[e] Minnan Normal University, Zhangzhou, 363000, China

ARTICLE INFO

Article history:
Received 30 December 2022
Received in revised form
25 September 2023
Accepted 27 September 2023

Keywords:
Temperature
Theoretical plate number
Breakthrough volume
Frontal chromatographic theory
LSER

ABSTRACT

Effective monitoring of atmospheric concentrations is vital for assessing the Stockholm Convention's effectiveness on persistent organic pollutants (POPs). This task, particularly challenging in polar regions due to low air concentrations and temperature fluctuations, requires robust sampling techniques. Furthermore, the influence of temperature on the sampling efficiency of polyurethane foam discs remains unclear. Here we employ a flow-through sampling (FTS) column coupled with an active pump to collect air samples at varying temperatures. We delved into breakthrough profiles of key pollutants, such as polycyclic aromatic hydrocarbons (PAHs), polychlorobiphenyls (PCBs), and organochlorine pesticides (OCPs), and examined the temperature-dependent behaviors of the theoretical plate number (N) and breakthrough volume (V_B) using frontal chromatography theory. Our findings reveal a significant relationship between temperature dependence coefficients (K_{TN}, K_{TV}) and compound volatility, with decreasing values as volatility increases. While distinct trends are noted for PAHs, PCBs, and OCPs in K_{TN}, K_{TV} values exhibit similar patterns across all chemicals. Moreover, we establish a binary linear correlation between log (V_B/m^3), 1/(T/K), and N, simplifying breakthrough level estimation by enabling easy conversion between N and V_B. Finally, an empirical linear solvation energy relationship incorporating a temperature term is developed, yielding satisfactory results for N at various temperatures. This approach holds the potential to rectify temperature-related effects and loss rates in historical data from long-term monitoring networks, benefiting polar and remote regions.

1. Introduction

Persistent organic pollutants (POPs) are particularly concerning due to their persistence, high toxicity, and bioaccumulation [1]. Polycyclic aromatic hydrocarbons (PAHs) are not strictly defined as POPs but are often studied alongside POPs due to their ubiquitous and pervasive toxic effects. Considering their volatility, POPs (including PAHs) belong to a group of semi-volatile organic compounds (SOCs). Once discharged into the environment, SOCs can be dynamically distributed between the gas phase, particulate phase, and other surface media, then eventually distributed among the atmosphere [2], water [3], soil [4], sediment [5], and biota [6]. Compared with other SOCs, the relatively longer atmospheric half-lives help POPs migrate with airflow diffusion [7] over long distances to condense in remote regions. With the decrease in temperature due to temperature gradients in latitudinal or vertical scales, SOCs will transfer from the gas phase to the particulate phase or surface medium, eventually concentrated over polar regions through “global fractionation” and “cold trapping” [8,9]. Thus, the

* Corresponding author. Institute of Urban Environment, Chinese Academy of Sciences, Xiamen, 361021, China.
E-mail address: hxiao@iue.ac.cn (H. Xiao).

https://doi.org/10.1016/j.ese.2023.100327

release of POPs into the environment raises a series of environmental and ecological problems [10], and their impacts on those fragile polar ecosystems may be disastrous. To work towards a POPs-free future, the Stockholm Convention on POPs was signed in 2001 and ratified in 2004. To evaluate the effectiveness of the treaty and other control measures, the globe monitoring plan (GMP) was implemented, tasked with the aggregation of data from existing monitoring networks [11]. Within the framework of GMP, atmospheric monitoring has assumed a pivotal role, given that the atmosphere serves as the principal and highly efficient medium for long-range transport (LRT). It not only provides insight into LRT and the persistence of chemicals but is also crucial for estimating emission factors and risk assessments [12,13]. The accurate measurement and evaluation of POPs in the atmosphere pose considerable challenges, particularly due to their prevalence at exceedingly low concentrations, notably in polar regions. With the continuous progress of instrumental technology in recent years, the efficiency of sampling technology has become the bottleneck of precise analysis.

High-volume active pumps with polyurethane foam as sampling media remain the prevailing and widely accepted quantitative sampling method [14,15]. Several long-operating atmospheric monitoring networks, such as the Arctic Monitoring and Assessment Programme (AMAP) and the Great Lakes Integrated Atmospheric Deposition Network (IADN), are rooted in this methodology [16,17]. As a necessary supplement, some economic, convenient, and semi-quantitative passive sampling techniques are also developed and applied for rough spatial-temporal comparison in large-scale or long-term studies [18,19]. However, studies on the effect of environmental factors and sampling conditions, such as temperature and sampling volumes, on the accuracy of sampling, sampling rate, and capacity remain limited both for active and passive sampling methods [20]. It often occurs that samples of volatile compounds have to be discarded due to severe breakthroughs during sampling [14,19]. In order to rectify the impact of breakthroughs on sampling, some studies have also attempted to explore the relationship between the back-to-front PUF (PUF 2/PUF 1) ratio [21] or partitioning between PUF and the gas phase and fractional collection efficiencies [22]. In recent years, a novel hybrid sampling technique known as the flow-through sampler (FTS) has emerged, using an active sampling mechanism without reliance on electrical power [23–25]. It has been successfully applied in extremely remote areas, such as the Arctic, Antarctic, and Qingzang Plateau [26–29]. FTS is a novel atmospheric sampler that uses wind energy to carry the flow of POPs through the polyurethane foam (PUF) sampling column. Then, the atmospheric concentration of the target compounds can be quantified by evaluating the sampling volume and adsorbed compound mass. Field tests have demonstrated that FTS is suitable for quantitative study on a wide range sampling of POPs. Furthermore, empirical equations have been derived to estimate the impacts of environmental conditions, such as temperature, on the breakthrough level of each sample. However, it is imperative to acknowledge a pertinent concern associated with long-term field observations. The instability of various environmental factors can introduce uncertainties into the data obtained from empirical equations [22].

As mentioned before, the variances in the properties and distributions of chemicals caused by temperature differences across diverse regions are the intrinsic driving force of the global distillation of POPs. Temperature also significantly affects the interaction between compounds and the stationary phases, hence affecting the penetration behavior of target compounds in the sample adsorption column during the atmospheric sampling process [21,25,30–32]. Given the substantial temperature differentials between polar and non-polar regions, it is important to study the effect of temperature on the sampling of POPs. So far, few studies have been carried out to quantify the impact of temperature on the breakthrough behavior of adsorption columns [30,33].

In order to improve the accuracy of atmospheric sampling and quantitatively describe the environmental behavior of POPs, it becomes imperative to conduct investigations into the adsorption characteristics of the target compounds within active sampling columns under different environmental conditions. In this study, we use an FTS sampling column connected with an active sampling pump to collect atmospheric pollutants in different seasons and temperatures. The FTS sampling column was used for its convenient design [23,24]. The influence of temperature on the penetration behavior of compounds in sampling PUF column was further quantitatively investigated using front chromatographic theory. These results not only provide theoretical guidance for the correction of loss rates during FTS sampling at different temperatures but also give insights into understanding the mechanism of active sampling and the ideal use of active samplers to achieve maximum sampling efficiency.

2. Materials and methods

2.1. Sampling procedure

Our research was conducted in Ningbo, situated along the southeastern coast of China, south of the Yangtze River Delta, ranked as the world's third-largest port city. The research site was located on the roof of the Ningbo Urban Environment Observation and Research Station (NUEORS, 29.75° N, 121.9° E), Chinese Academy of Sciences, Chunxiao Town, Beilun District, Ningbo, with an altitude of about 15 m. More detailed information on this site has been mentioned in a previous study [34].

The FTS sample cylinder contained seven P10z PUF (a type of polyester-polyurethane foam with a density of 0.0304 g cm^{-3} and a porosity of 10 pores per inch) discs with a diameter of 10.5 cm and thickness of 2.54 cm (Fig. 1a and b, purchased from Pinta Industry Inc., Minneapolis, MN 55430, USA, http://www.pinta-industry.com), The total length of the sampling column is 17.8 cm with a cross-sectional area of 8.66×10^{-3} m^2. The FTS sampling column is connected with an Anderson 8-grade particulate matter sampler (series 20-800, Thermo Scientific, USA) [35] with a customized adaptor (Fig. 1a), which operated at a flow rate of 28.3 L min^{-1}, equivalent to an airflow velocity of about 0.054 m s^{-1} through the cross-section of FTS sampling tube. The sampler was equipped with front and rear stainless steel screens, strategically designed to act as protective barriers against the ingress of insects or large particles during the sampling process. Before exposure, the disks were precleaned with water, followed by sequential washes in methanol, *n*-hexane:acetone (1:3), *n*-hexane:acetone (3:1), and acetone using an Accelerated Solvent Extractor (ASE 350). More details of the extracting conditions are described in previous research [36]. During the experiment, 60 groups of samples and 420 PUF discs were collected from October 2016 to October 2017. Table 1 shows samples taken during different seasons, with average temperatures of each sampling period about 5, 10, 20, and 30 °C. To maximize the likelihood of exceeding the instrument's quantitative detection limit, the sampling was divided into three groups: one day, four days, and eight days. A field blank was taken for each sample, involving the exposure of a PUF disk to air during sample installation. Subsequently, these discs were sealed in the original jar and placed beside the FTS for the sampling length.

2.2. Sample extraction and quantification

The PUF disks from the flow-through sampler and the front and back PUF of the pumped samples were extracted individually by

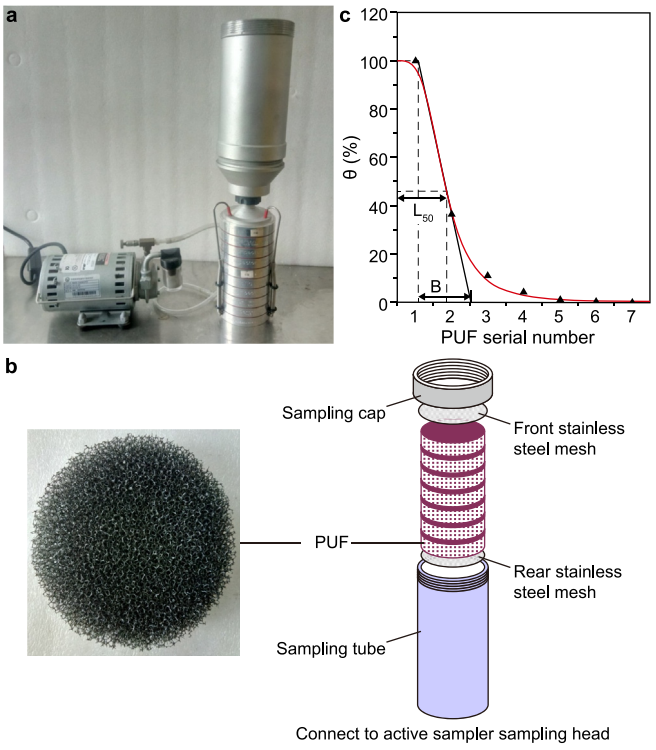

Fig. 1. a, FTS sampling tube connected with an Anderson 8-stage sampler. **b**, FTS sampling tube and PUF. **c**, The logistic curve.

ASE with *n*-hexane and acetone (3:1). The extracts were reduced in a rotary evaporator, transferred to a vial, and reduced under a gentle nitrogen flow. The sample was exchanged for isooctane before instrumental analysis. More details of the sample handling information are described in a study by Xiao et al. [24]. Mirex (100 ng) was added as an internal standard to correct for volume differences.

Samples were analyzed for 54 polychlorinated biphenyl (PCB) congeners, 23 organochlorine pesticides (OCPs), and 16 polycyclic aromatic hydrocarbons (PAHs) using standard mixtures from AccuStandard, Inc. (New Haven, CT, USA) and Wellington laboratories (Guelph, ON, Canada). Deuterated internal standards of PAHs (acenaphthene-d10, pyrene d10, and benzo [e] pyrene d12) were purchased from Wellington laboratories (Guelph, ON, Canada). Quantification was achieved with a 7890b/5977a gas chromatograph (GC) (Agilent, USA) equipped with a splitless injector and a mass spectrometer operating in electron impact-selected ion monitoring mode. GC conditions have been described elsewhere [11]. The temperature program of the GC oven was adjusted as follows. An initial temperature of 130 °C was maintained for 0.5 min. Subsequently, the temperature was ramped up at a rate of 10 °C min^{-1} until reaching 240 °C, followed by a more rapid increase of 20 °C min^{-1} to attain 325 °C. The final temperature setting was held steady for 5 min.

2.3. Quality assurance (QA)/quality control (QC)

The evaluation of chemical recovery in our analytical method involved spiking two clean PUF disks with the working standard containing all PCB, OCP, and PAH congeners (20 ng of each congener) and treating them as actual samples. Results showed good recoveries ranging from 69% to 105%, aligning favorably with previous air sampling studies in the laboratory using the same methodology [24]. Recovery factors were not applied to any of the data reported below. Solvent blanks and field blanks for PUF were typically less than 8% of the sample amounts, except for four chemicals with very low abundance, namely PCB-185, PCB-201, PCB-209, and benzo (g, h, i) perylene (these four compounds were eventually ignored due to the low frequency detected). All the amounts reported for the samples are corrected for field blanks. We employed two-thirds of the instrumental detection limit as a correction factor for undetectable compounds in those blanks. The instrumental detection limit was established as the quantity at which the signal-to-noise ratio reached a value of 3, and comprehensive information can be found in Supporting Information Schedule 7.

2.4. Data analysis

This study used SPSS 24.0 (IBM, USA) and Origin 9.0 (Originlab, USA) for data processing and drawing.

2.5. Frontal chromatography theory

Assuming that the concentrations of various compounds in the air remain relatively constant during each sampling period, the sampling PUF discs could be treated as a frontal gas chromatography column with a few theoretical plates [37]. According to frontal chromatographic theory, the theoretical plate number of the sampling assembly (N) can be determined from the ratio between the thickness of the foam at the 50% breakthrough point or the half peak width (L_{50}) of the compound in the adsorption column and the line segment B, where B is related to the tangent at the half peak width of the breakthrough curve (Fig. 1c) (equation (1)) [38,39]. According to the shape and boundary conditions of the breakthrough curve, Xiao et al. (2007) [23] first introduced the method of logistic curve fitting to describe the breakthrough curve of a compound on the sampling column, where θ is the chemical amount trapped on each PUF as a percentage of that trapped on the first PUF plug, and L is the overall PUF thickness (equation (2)). After a series of derivations, the N of a sampling column is only related to the fitting parameter q of the logistic regression (equation (3)) [23]. This non-linear fitting result can ensure more consistent results and accurate data than manually drawing the measurement curve. Detailed information parameters of L_{50}, B, q, N, and θ are described in Ref. [23].

$$N = 2\pi\left(\frac{L_{50}}{B}\right)^2 \quad (1)$$

Table 1
Temperature variations for different sampling times at a constant sampling rate of 28.3 L min^{-1} (equivalent to an airflow rate of 0.054 m s^{-1} through the cross-section of the FTS sampler).

Sample group	A	B	C	D	E	F	G	H	I	J	K	L
Sampling time (d)	1	1	1	1	4	4	4	4	8	8	8	8
Average temperature (°C)	5.3 ± 2.4	10.4 ± 3.2	20.1 ± 3.6	30.5 ± 4.5	5.2 ± 3.7	10.3 ± 4.3	20.4 ± 5.1	30.2 ± 4.9	5.4 ± 4.5	10.2 ± 5.3	20.4 ± 6.4	30.6 ± 5.1
Temperature range (°C)	3–11	4–19	17–24	28–32	−1 to 11	3–18	11–25	27–36	−2 to 12	0–19	11–26	27–38

$$\theta(\%) = f(L) = \frac{100}{1 + \left(\frac{L}{L_{50}}\right)^{q}} \quad (2)$$

$$N = \frac{\pi q^2}{8} \quad (3)$$

3. Results and discussion

3.1. Influence of temperature on the non-linear fitting curve

The logistic regression of breakthrough behavior of three selected PAHs, OCPs, and PCBs on the FTS sampling columns was shown in Fig. 2, while similar results were given in Figs. S1–S3 for other chemicals. At the same sampling time and volume, the front edge of the breakthrough curve of all monitored target compounds gradually moved from the front to the end with increasing temperature, and L_{50} increased in turn. At the same temperature, with increasing sampling time and volume, the moving distance of the same compounds on the PUF columns was larger. The volatility of the compounds decreased with increasing molecular weight, and the migration distance of the compounds on the adsorption column gradually decreased. For highly volatile compounds, such as fluorene (Flu) and hexachlorocyclohexane (HCH), breakthroughs occurred easily, especially at higher temperatures and larger sampling volumes. The θ value of each disc on the adsorption column was greater than 50% since the adsorption capacity of the PUF adsorption columns was limited, aligned with the previous results of Huang et al. [40]. The non-linear fitting effect of gaseous

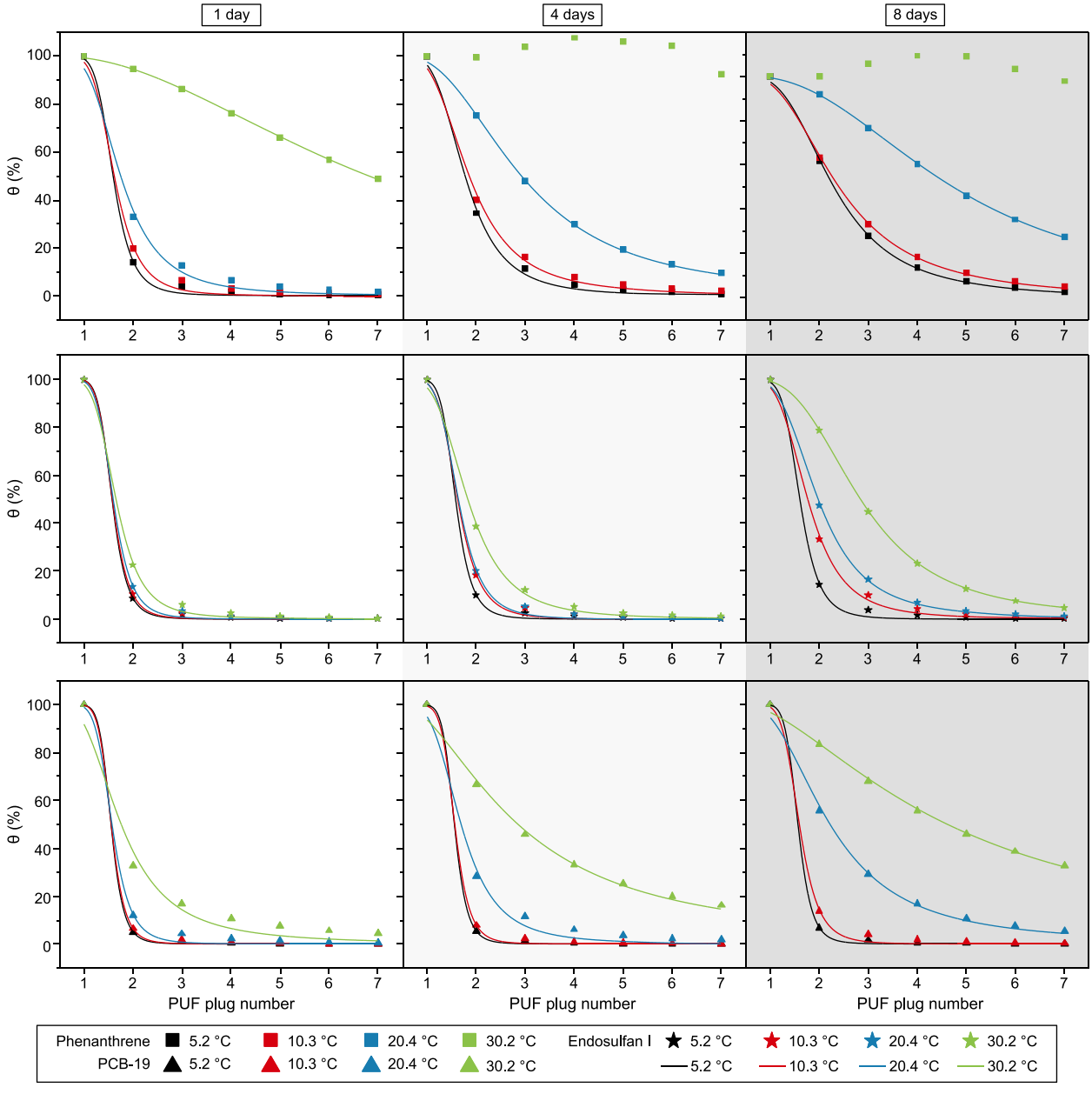

Fig. 2. The breakthrough curves of typical compounds at different temperatures and sampling times.

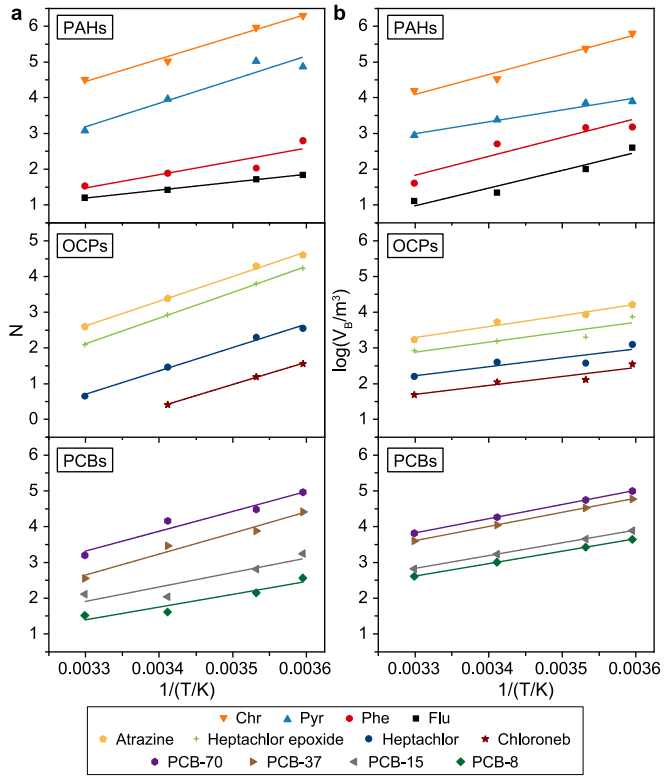

Fig. 3. The effect of temperatures on N (**a**) and log (V_B/m^3) (**b**) of compounds in the FTS sampling column.

compounds with high volatility (log (P_L/Pa) > −1.5) was poor. Although statistical fitting can still be performed, the extrapolated L_{50} and q results generally have high uncertainty. In these cases, the corresponding data was ignored in this study; nevertheless, this data retains significant utility. These PUF discs can be treated as equilibrium-state passive air samplers, and the absolute value of their sampling amount can provide information on the PUF/air partitioning coefficient, which will be explored in depth in subsequent studies. For others, the L_{50} and q values were obtained from the fitting curve, and the N values could be further calculated. The results are listed in Table S1.

The breakthrough volume V_B of the sampling column could be obtained by plotting the sampled air volume against the regression parameter L_{50} and extrapolating the corresponding regression lines to the entire sampling column length, as described in Xiao et al. [23]. The relevant results are given in Fig. S4. However, due to the limitation of PUF disc thickness, when applying linear regression to relate sample volume to the L_{50} values of different compounds, the intersection point with the x-axis (column length) does not coincide with the origin. Instead, it consistently converges at the midpoint of the initial disc. The accuracy of L_{50} and V_B was limited; the relative change trend for all chemicals should be credible even if the absolute value may have certain systematic errors.

3.2. Effect of temperature on theoretical plate number and breakthrough volume

Previous studies showed that the penetration of the target compound through the PUF adsorption column mainly depended on the volatility of the compound and the sampling volume [41–45]. In plate theory, the theoretical plate number is introduced as the index to measure chromatographic column efficiency. Fig. 3

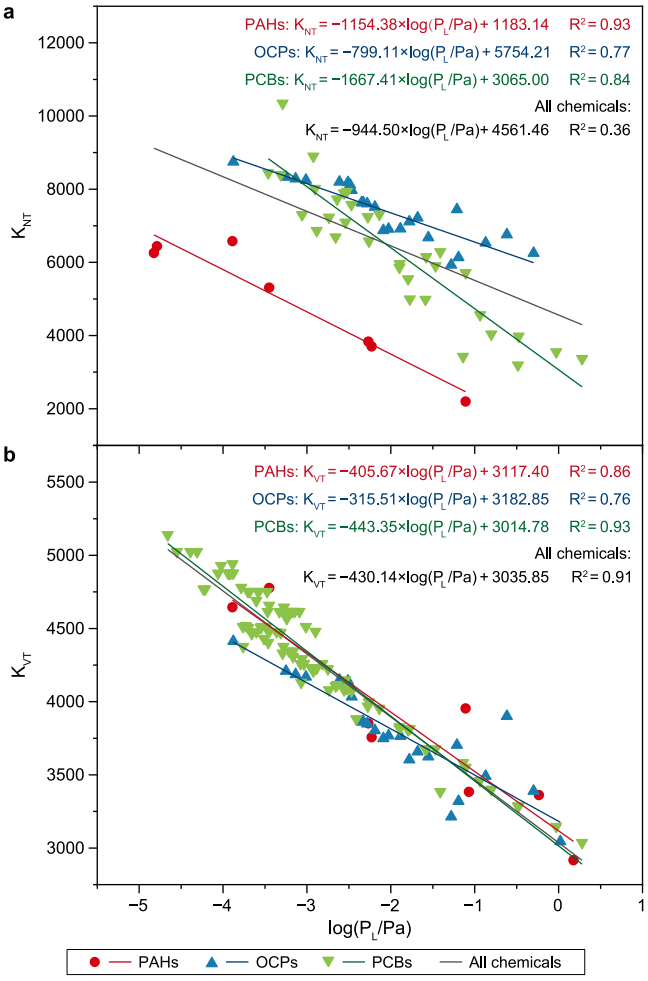

Fig. 4. The relationship between log (P_L/Pa) and the temperature dependence coefficients (the slope of the linear regression between the corresponding physicochemical property and 1/(T/K)) for N (**a**) and log (V_B/m^3) (**b**).

shows the relationship between N of each compound through the sampling column at different temperatures and 1/(T/K). A good linear relationship exists between the 1/(T/K) and N for different compounds. As 1/(T/K) increases, the theoretical plate number increases, resulting in a decrease in N values with increasing temperature. This phenomenon aligns with previous research results [23,38,39,46]. Since the magnitude of the N value reflects the strength of the interaction between the compound and the sampling column, the slope obtained from the temperature dependence reflects the temperature's impact on the N of the compound (Table S2). For a certain sampling column, these slope differences may be determined by the physical and chemical properties of the compounds. Consequently, we conducted an analysis to explore the relationship between the obtained temperature-dependent slopes and each compound's physical and chemical properties. Similarly, the bottom part of Fig. 3 also shows the temperature dependence of the breakthrough volume (log (V_B/m^3)) of the sampling column to each compound during sampling. Notably, a robust linear relationship between the temperature and log (V_B/m^3) is evident through linear fitting. Saturated supercooled liquid vapor pressure (P_L) is an essential physical and chemical parameter of compounds, characterizing their volatility. This parameter is often used in linear free energy correlation (LFER) research. Numerous research shows that the logarithm of a compound's P_L has an apparent linear

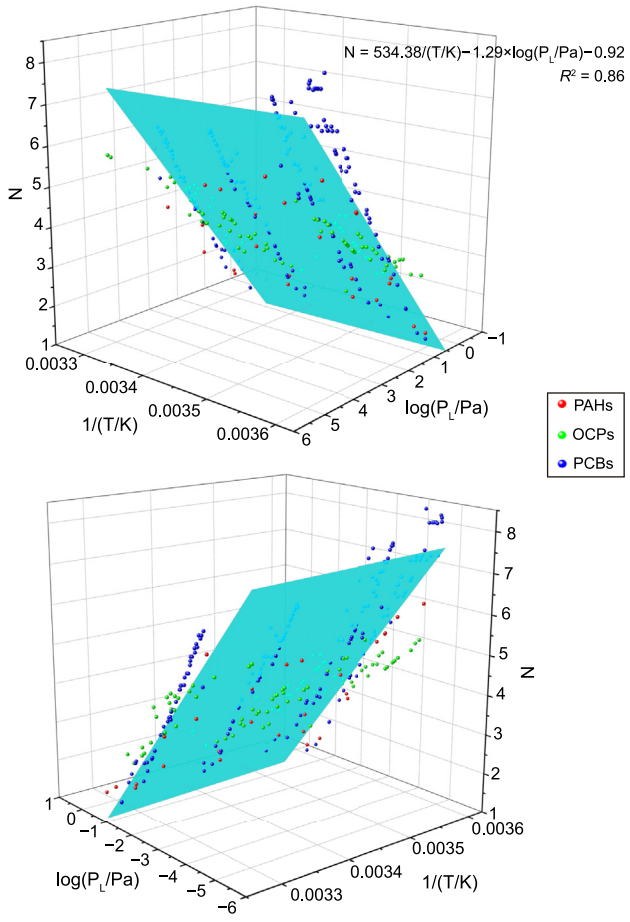

Fig. 5. The correlation between log (P_L/Pa), 1/(T/K), and N.

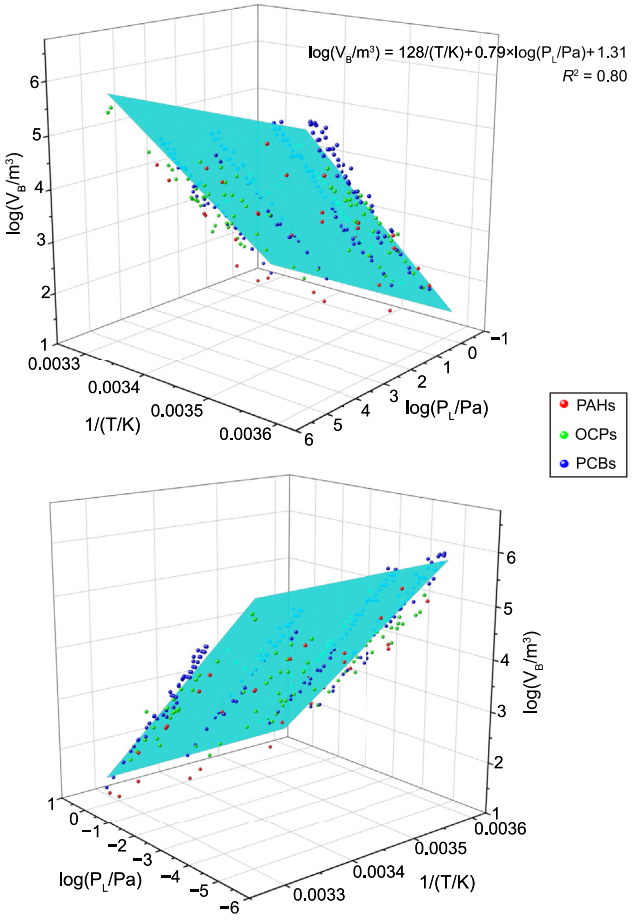

Fig. 6. The correlation between log (P_L/Pa), 1/(T/K), and log (V_B/m^3).

relationship with the reciprocal of absolute temperature or log (P_L/*Pa*) = m_L/(T/*K*) + b_L. The relevant parameters of the target PAHs, OCPs, and PCBs could be obtained from the reference [47–49]. According to the average temperature of the sampling process, the saturated vapor pressure of the supercooled liquid of each compound under the experimental conditions can be calculated. Octanol-air partition coefficient (K_{OA}) was another often used descriptor for volatility. Some references indicate that K_{OA} is a preferred alternative to P_L for describing the partitioning of non-polar organic compounds between the gas phase and various surface media. However, as shown in the previous study by Xiao and Wania [50], P_L and K_{OA} are highly correlated. Therefore, it is impossible to determine the superiority of one parameter over the other with current precision, and poly-parameter LSER is more advantageous than the single parameter-linear free energy relationships. Similar results using K_{OA} instead of P_L as a volatility descriptor are given in the Supporting Information (Figs. S4–S6) for comparison.

The volatility of compounds is closely related to their gas phase/particle phase partition behavior [51,52]. PAHs with log (P_L/Pa) > −1.5 are mostly present in the gas phase, while PAHs with log (P_L/Pa) < −5 are mostly present in the particle phase [53,54]. The penetration of compounds completely distributed in a particulate state mainly depends on the interception effect of the sampling medium on particulate matter; however, the logistics fitting curve can get with the distribution between the mobile phase and the stationary phase of chromatography, and is not suitable for the interception effect of the sampling column on particulate matter.

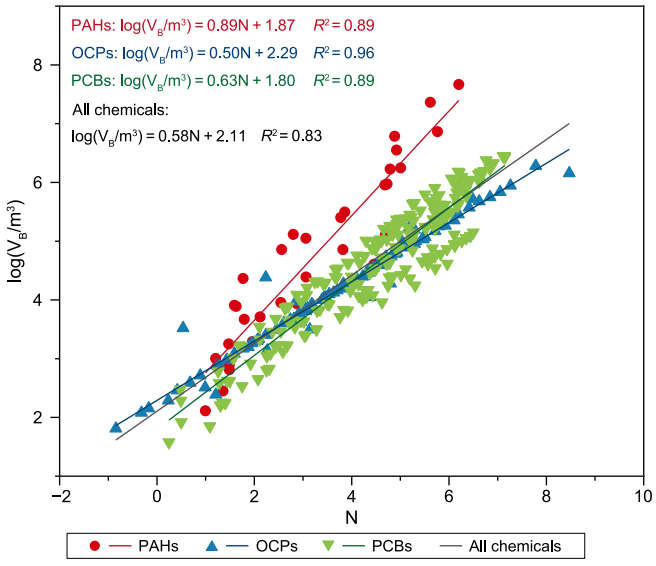

Fig. 7. The relationship between the log (V_B/m^3) and N is affected by different temperatures.

Therefore, the collection effect of the sampling column on compounds mainly distributed in the particulate phase was beyond the scope of this study.

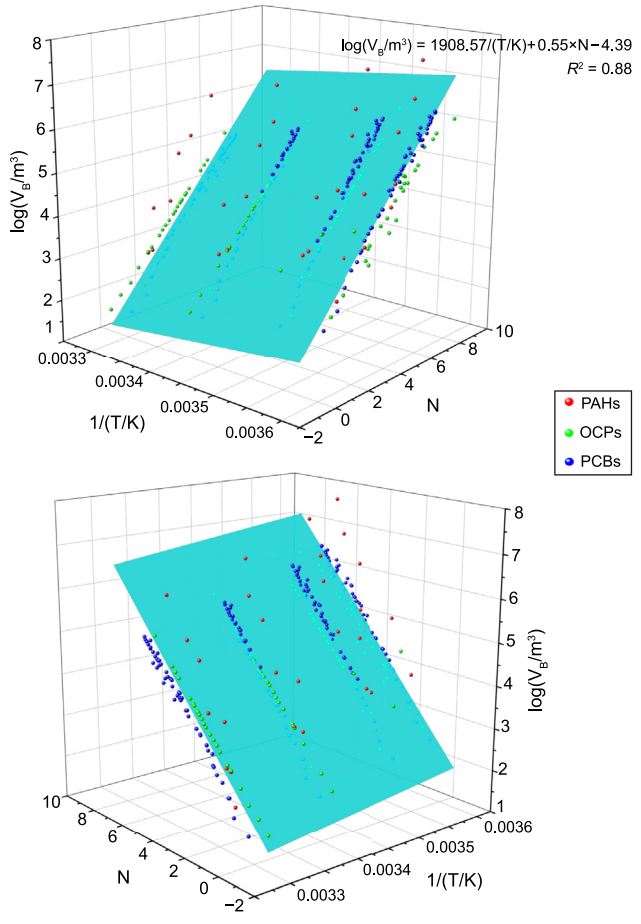

Fig. 8. The relationship between N and log (V_B/m^3) of different compounds in different temperatures.

The correlation between the slope of the theoretical plate number of the FTS sampling column for POPs (the slope of the linear fitting of 1/(T/K) and N, denoted as K_{NT}) and the log (P_L/Pa) of the compound is shown in Fig. 4a. The K_{NT} value gradually increased with the decrease of log (P_L/Pa) of the compound. This trend indicates that the theoretical plate number of the sampling adsorption column for the less volatile POPs was more sensitive to temperature variations. The K_{NT} of OCPs and PCBs with low volatility was similar, while the temperature response of OCPs and PCBs was significantly higher than that of PAHs with similar volatility. Linear fitting was carried out for each group of compounds and then combined, with detailed results provided in Table S2.

The linear relationship between the slope (K_{VB}) of each linear fit (Table S3) and log (P_L/Pa) is shown in Fig. 4b. Volatility can explain the change in the breakthrough volume of each compound in the sampling column affected by temperature. The trend of temperature influence on the breakthrough volume of the three types of compounds (PAHs, OCPs, PCBs) was consistent. Then, it is possible to accurately estimate the breakthrough volume of chemicals on the FTS column based on its volatility.

Considering the influence of temperature and compound volatility (log (P_L/Pa)) on the N of the sampling column on the compound, the result of the binary linear regression is shown in Fig. 5. The corresponding fitting surface can describe the change of N of PAHs and PCBs. However, the fitting performance for OCPs with different compound properties is relatively poor. This implies

Table 2
Empirical LSER correlations with $1/(T/K)$ term for fitting of N of PAHs, OCPs, PCBs, and all compounds at different temperatures, and the corresponding statistical test results.

LSER regression coefficients	Total				PAHs				OCPs				PCBs			
	Average	Standard error	T value	P value	Average	Standard error	T value	P value	Average	Standard error	T value	P value	Average	Standard error	T value	P value
c	−3.27	0.19	−17.21	0	−3.17	0.39	−8.12	0	−0.99	0.31	−3.25	0.0026	−3.01	0.63	−4.75	0
T	702.87	51.83	13.56	0	670.57	91.83	7.30	0	223.41	81.22	2.75	0.0095	894.73	46.23	19.35	0
b	−0.38	0.04	−9.23	0	2.76	4.06	0.68	0.51	−0.24	0.058	−4.18	0.00019	−3.19	1.23	−2.59	0.011
L	0.18	0.013	13.79	0	−0.05	0.26	−0.20	0.85	0.12	0.14	5.51	0.00001	0.12	0.035	3.37	0.0011
e	−0.15	0.030	−4.90	0	−0.11	0.13	−0.89	−0.39	−0.065	0.34	5.451	0.0005	−0.55	0.67	−0.082	0.41
S	0.11	0.042	2.63	0.0094	0.83	0.72	1.14	0.27	0.041	0.23	−5.58	0.009	0.64	0.53	1.21	0.23

that not only does volatility affect the *N* value of the compound (or the strength of the interaction between the adsorption column and the compound), but other physical and chemical properties might play an important role.

Fig. 6 is a three-dimensional relationship diagram of $1/(T/\mathrm{K})$, log (P_L/Pa), and log (V_B/m^3). The uniform binary regression fitting for the three groups of compounds, including PAHs, OCPs, and PCBs, obtained satisfactory results (R^2 is 0.80) (equation (4)), in which log (V_B/m^3) and $1/(T/\mathrm{K})$ are positively correlated, while log (V_B/m^3) and log (P_L/Pa) are negatively correlated. This result is consistent with that of Xiao et al. (2007) [23], and the breakthrough volume (V_B) of these three types of compounds can be estimated simply based on temperature and their volatilities.

$$\log\left(V_B/\mathrm{m}^3\right)=\frac{128}{(T/\mathrm{K})}-0.79\times\log(P_L/\mathrm{Pa})+1.31\left(R^2=0.80\right) \quad (4)$$

3.3. Relationship between theoretical plate number and breakthrough volume

Based on the above analysis and comparison, both *N* and log (V_B/m^3) have an excellent linear relationship with the temperature and volatility of compounds. Fig. 7 shows the relationship between the theoretical plate number and log (V_B/m^3) on the FTS sampling column. Significant linear correlations exist between these two parameters for three chemical groups. In particular, OCPs have the best linear relationship. For PAHs and PCBs, the correlation at different temperatures shifts significantly, resulting in a wide band distribution of data points. In general, the changing trends between *N* and log (V_B/m^3) of the three chemical classes are consistent, but the relationship between PAHs and the other two types of substances is slightly different.

Binary linear fitting of $1/(T/\mathrm{K})$, *N*, and log (V_B/m^3) was carried out (Fig. 8) for all chemicals analyzed, and the fitting equation is given in equation (5) ($R^2 = 0.88$). The close correlation between these two parameters suggests the potential for mutual conversion as required.

$$\log\left(V_B/\mathrm{m}^3\right)=\frac{1908.57}{(T/\mathrm{K})}+0.55N-4.39 \qquad \left(R^2=0.88\right) \quad (5)$$

3.4. Linear solvation energy relationships (LSER) for predicting theoretical plate number at different temperature

As discussed previously, volatility may not be the only physical-chemical property that affects the partitioning behaviors of chemicals on a PUF sampling column. Poly-parameter linear free energy relation (PP-LFER) has significant advantages over single-parameter linear free energy relation (SP-LFER) in predicting the distribution behavior of various organic compounds. It is often used to study the distribution system and distribution coefficient of compounds in different environments [50,55]. Many studies use the LSER formula to predict interphase partition coefficients [56–60]. However, most of these researches did not involve properties at different temperatures. Thus, this study added a reciprocal term of temperature to LSER to form an empirical equation to describe the temperature effect.

$$SP=l\times\log L_{16}+eE+sS+aA+bB+\frac{t}{T}+c \quad (6)$$

In equation (6), *SP* represents a property, here as *N*. Except for *T* for temperature in Kelvin, Abraham parameters (can be obtained from UFZ-LSER database, http://www.ufz.de/lser, [61]), logL_{16}, *E*, *S*, *A*, and *B* are empirical descriptors of the solute for cavitation, excess molar refraction, dipolarity/polarizability, hydrogen bond donor, and hydrogen bond acceptor of the solute, respectively. The multiple linear regression constants *l*, *e*, *s*, *a*, *b*, and *c* reflect the properties of the sampled medium for various corresponding interactions.

Table 2 lists the results of LSER regression with this temperature term for the three groups and all compounds, which included the regression coefficient, standard deviation, *t*-test result, and *p*-value of each parameter. It should be noted that whether all compounds are considered as a whole or the three groups are analyzed separately, the *t*-test results of multiple linear regression show that the temperature term $(1/(T/\mathrm{K}))$ always contributes significantly to *N*. The reciprocal of temperature was positively correlated with *N* of the compound, which is consistent with the results of Xiao et al. [25]. The influence of temperature on *N* of the compounds of OCPs was less than that of PAHs and PCBs, which the smaller interaction between chemical bond structures in OCPs may cause. Since the PAHs, PCBs, and OCPs analyzed in this study are not strong hydrogen bond donors, for all chemicals, all other parameters but term *A* in the LSER equation significantly affect *N* of contaminants on the FTS sampling column. Regarding the interactions between chemicals and PUFs affecting *N*, we observe the following ranking from strongest to weakest influence: cavitations > hydrogen bond receptors > dispersion interaction due to excess molar refraction > dipole interactions. Interestingly, when PAHs are considered separately, the reciprocal of temperature is the only physical quantity other than the intercept that significantly correlates with the theoretical plate number of PAHs on the FTS sampling column. This may be because PAHs used for analysis are a small group of non-polar compounds, and strong autocorrelations exist between Abraham's parameters and $1/(T/\mathrm{K})$.

Compared with the previous equation in Ref. [25], our study offers a notable improvement by utilizing a consistent sampling rate, resulting in significantly improved equation fitting. However, this study did not consider the impacts of sampling rate/wind speeds. As previous studies pointed out, it is possible to estimate the breakthrough level *b*, defined as the fraction of the total mass of the analyte eluted from a sampling column if the *N* and V_B are known [26,37]. Therefore, with the knowledge of the temperature influence of PAHs, PCBs, and OCPs on penetration performance on the PUF sample column, the loss rate of any chemical can be accessed based on its physical-chemical properties and the sampling volume. By replicating similar analyses on specific sampling media following the experimental design of this study, historical data could be re-evaluated after correction for the breakthrough. Furthermore, the ideal sampling volume could be estimated before each sampling campaign for any chemical of interest. The accuracy and application scope of the equation may be further improved based on the influence of other environmental factors on the performance of the sampling column to be discussed later, including variables such as the sampling rate and wind speed.

4. Conclusion

This study aims to unravel the impact of temperature variations on the compound's penetration characteristics within the adsorption medium. To achieve this, we conducted a comprehensive investigation across various seasons, connecting an active sampling pump with the flow-through sampling column. The key findings from our study are outlined below :

(1) Temperature exerts a substantial influence on the theoretical plate numbers of compounds on the sampling adsorption column. The corresponding fitting slope (K_{TN}) is significantly related to the volatility of the compounds: the less the

volatility, the greater the influence of temperature changes on the N of the sampling column. The influence on several volatile OCPs was significantly greater than PAHs and PCBs. Further LSER analysis considering the influence of temperature showed that the reciprocal of temperature is positively correlated with N, and the fitting effect ($R^2 = 0.85$) is better upon adding the temperature term.

(2) There is also a significant linear relationship between $1/(T/\mathrm{K})$ and $\log(V_B/m^3)$. The slope of the breakthrough volume of different compounds on the sampling column affected by temperature (K_{TN}) is significantly correlated with the compound's volatility ($\log(P_L/\mathrm{Pa})$). The effect of temperature on the breakthrough volume of low-volatile compounds is greater than that of volatile compounds.

(3) A good correlation exists between N and $\log(V_B/m^3)$, with temperature playing a pivotal role in shaping this association. Therefore, the loss rate due to breakthrough, originally calculated based on N and relative retention (expressed as volume-based, the ratio of sampling volume to the V_B), can be simplified by this correlation. As a result, the ideal sampling volume of compounds at a specific temperature and within the acceptable range of outflow rate can be estimated.

(4) For chemicals with serious breakthroughs, the few PUF discs in front of the FTS sampling column can be treated as equilibrium-state passive air samples. The temperature dependence of the partitioning of POPs between PUF media and air holds promise for future research endeavors.

CRediT authorship contribution statement

Qiu-Liang Cai: Writing - Original Draft, Writing - Review & Editing, Methodology, Formal Analysis. **Cen-Yan Huang:** Writing - Review & Editing, Software, Methodology, Formal Analysis, Visualization. **Lei Tong:** Methodology, Writing - Review & Editing, Validation, Visualization. **Ning Zhong:** Formal Analysis, Resources, Data Curation. **Xiao-Rong Dai:** Writing - Review & Editing, Validation. **Jian-Rong Li:** Investigation, Data Curation. **Jie Zheng:** Writing - Review & Editing, Validation. **Meng-Meng He:** Resources, Project Administration. **Hang Xiao:** Conceptualization, Writing - Review & Editing, Supervision, Visualization, Funding Acquisition.

Declaration of competing interest

The authors declare that they have no known competing financial interests or personal relationships that could have appeared to influence the work reported in this paper.

Acknowledgments

This work was supported by the National Natural Science Foundation of China (No. 21976171, 41905115), the CAS Strategic Priority Research Program (XDA23020301), the Guangxi Key Research and Development Program (GuikeAB21220063), the Ministry of Science and Technology of the People's Republic of China (2016YFE0112200), and Guangxi First-class Disciplines (Agricultural Resources and Environment). The authors also want to thank EditSprings (https://www.editsprings.cn/) for the expert linguistic services provided.

Appendix A. Supplementary data

Supplementary data to this article can be found online at https://doi.org/10.1016/j.ese.2023.100327.

References

[1] K. Takagi, Study on the biodegradation of persistent organic pollutants (POPs), J. Pestic. Sci. 45 (2) (2020) 119–123, https://doi.org/10.1584/jpestics.J19-06.
[2] K.C. Jones, Persistent organic pollutants (POPs) and related chemicals in the global environment: some personal reflections, Environ. Sci. Technol. 55 (14) (2021) 9400–9412. https://pubs.acs.org/doi/10.1021/acs.est.0c08093.
[3] S.H. Lee, J.S. Ra, J.W. Choi, et al., Human health risks associated with dietary exposure to persistent organic pollutants (POPs) in river water in Korea, Sci. Total Environ. 470–471 (2014) 1362–1369, https://doi.org/10.1016/j.scitotenv.2013.08.030.
[4] G.L. Yuan, H.Z. Wu, S. Fu, et al., Persistent organic pollutants (POPs) in the topsoil of typical urban renewal area in Beijing, China: status, sources and potential risk, J. Geochem. Explor. 138 (2014) 94–103, https://doi.org/10.1016/j.gexplo.2014.01.001.
[5] S. Vauclin, B. Mourier, A.M. Dendievel, et al., Temporal trends of legacy and novel brominated flame retardants in sediments along the Rhne River corridor in France, Chemosphere (2021) 129889, https://doi.org/10.1016/j.chemosphere.2021.129889.
[6] F. Rigét, A. Bignert, B. Braune, et al., Temporal trends of persistent organic pollutants in Arctic marine and freshwater biota, Sci. Total Environ. 649 (2018) 99–110, https://doi.org/10.1016/j.scitotenv.2018.08.268.
[7] H. Kaupp, M.S. McLachlan, Atmospheric particle size distributions of polychlorinated dibenzo-p-dioxins and dibenzofurans (PCDD/Fs) and polycyclic aromatic hydrocarbons (PAHs) and their implications for wet and dry deposition, Atmos. Environ. 33 (1) (1999) 85–95, https://doi.org/10.1016/S1352-2310(98)00129-0.
[8] F. Wania, Y.S. Su, Quantifying the global fractionation of polychlorinated biphenyls, Ambio 33 (3) (2004) 161–168, https://doi.org/10.1639/0044-7447(2004)033[0161:QTGFOP]2.0.CO;2.
[9] F. Wania, J.N. Westgate, On the mechanism of mountain cold-trapping of organic chemicals, Environ. Sci. Technol. 42 (2008) 9092–9098, https://doi.org/10.1021/es8013198.
[10] M. Pirsaheb, S. Zadsar, S.O. Rastegar, et al., Bioleaching and ecological toxicity assessment of carbide slag waste using Acidithiobacillus bacteria, Environ. Technol. Innov. 22 (2021) 101480, https://doi.org/10.1016/j.eti.2021.101480.
[11] S. Schanzer, E. Kröner, G. Wibbelt, et al., Miniaturized multiresidue method for the analysis of pesticides and persistent organic pollutants in non-target wildlife animal liver tissues using GC-MS/MS, Chemosphere 130434 (2021), https://doi.org/10.1016/j.chemosphere.2021.130434.
[12] H. Hung, M. MacLeod, R. Guardans, et al., Toward the next generation of air quality monitoring: persistent Organic Pollutants (POPs), Atmos. Environ. 80 (2013) 591–598, https://doi.org/10.1016/j.atmosenv.2013.05.067.
[13] UNEP, Second global monitoring report, Global Monitoring Plan for Persistent Organic Pollutants under the Stockholm Convention Article 16 on Effectiveness Evaluation. UNEP/POPS/COP.8/INF/38 (2017) 129.
[14] L.F. Zhang, T. Zhang, D. Liang, et al., Assessment of halogenated POPs and PAHs in three cities in the Yangtze River Delta using high-volume samplers, Sci. Total Environ. 454–455 (2013) 619–626, https://doi.org/10.1016/j.scitotenv.2013.03.051.
[15] T.F. Bidleman, L. Melymuk, Forty-five Years of Foam: a retrospective on air sampling with polyurethane foam, Bull. Environ. Contam. Toxicol. 102 (4) (2019) 447–449, https://doi.org/10.1007/s00128-019-02591-4.
[16] F. Wong, H. Hung, H. Dryfhout-Clark, et al., Time trends of persistent organic pollutants (POPs) and chemicals of emerging Arctic concern (CEAC) in Arctic air from 25 years of monitoring, Sci. Total Environ. (2021), https://doi.org/10.1016/j.scitotenv.2021.145109.
[17] S.S. Buehler, R.A. Hites, Peer reviewed: the Great Lakes' integrated atmospheric deposition network, Environ. Sci. Technol. 36 (17) (2002) 354A–359A, https://doi.org/10.1021/es0224030.
[18] C. Chaemfa, J.L. Barber, K.S. Kim, et al., Further studies on the uptake of persistent organic pollutants (POPs) by polyurethane foam disk passive air samplers, Atmos. Environ. 43 (25) (2009) 3843–3849, https://doi.org/10.1016/j.atmosenv.2009.05.020.
[19] M.Y. Tominaga, C.R. Silva, J.P. Melo, et al., PCDD, PCDF, dl-PCB and organochlorine pesticides monitoring in São Paulo City using passive air sampler as part of the Global Monitoring Plan, Sci. Total Environ. 571 (2016) 323–331, https://doi.org/10.1016/j.scitotenv.2016.07.173.
[20] C.Y. Huang, W.P. Shan, H. Xiao, Recent advances in passive air sampling of volatile organic compounds, Aerosol Air Qual. Res. 18 (2018) 602–622, https://doi.org/10.4209/aaqr.2017.12.0556.
[21] T.F. Bidleman, M. Tysklind, Breakthrough during air sampling with polyurethane foam: what do PUF 2/PUF 1 ratios mean? Chemosphere 192 (2018) 267–271, https://doi.org/10.1016/j.chemosphere.2017.10.152.
[22] Y.N. Li, F. Wania, Partitioning between polyurethane foam and the gas phase: data compilation, uncertainty estimation and implications for air sampling, Environ. Sci. Proc. Imp. 23 (2021) 723–734, https://doi.org/10.1039/D1EM00036E.
[23] H. Xiao, H. Hung, T. Harner, et al., A flow-through sampler for semi-volatile organic compounds in air, Environ. Sci. Technol. 41 (1) (2007) 250–256, https://doi.org/10.1021/es062024x.
[24] H. Xiao, H. Hung, T. Harner, et al., Field testing a flow-through sampler for semi-volatile organic compounds in air, Environ. Sci. Technol. 41 (1) (2008) 2970–2975, https://doi.org/10.1021/es702741b.

[25] H. Xiao, H. Hung, Y.D. Lei, et al., Validation of a flow-through sampler for pesticides and polybrominated diphenyl ethers in air, Atmos. Environ. 43 (15) (2009) 2401–2409, https://doi.org/10.1016/j.atmosenv.2009.02.006.
[26] H. Xiao, S.C. Kang, Q.G. Zhang, et al., Transport of semi-volatile organic compounds to the Tibetan Plateau: monthly resolved air concentrations at Nam Co, J. Geophys. Res. Atmos. 115 (2010), https://doi.org/10.1029/2010JD013972.
[27] H. Xiao, H. Hung, F. Wania, et al., Field evaluation of a flow-through sampler for measuring pesticides and brominated flame retardants in the Arctic atmosphere, Environ. Sci. Technol. 46 (14) (2012) 7669–7676, https://doi.org/10.1021/es301481w.
[28] H. Xiao, L. Shen, Y.S. Su, et al., Atmospheric concentrations of halogenated flame retardants at two remote locations: the Canadian High Arctic and the Tibetan Plateau, Environ. Pollut. 161 (2012) 154–161, https://doi.org/10.1016/j.envpol.2011.09.041.
[29] S.M. Bengtson Nash, S.J. Wild, D.W. Hawker, et al., Persistent organic pollutants in the east Antarctic atmosphere: inter-annual observations from 2010 to 2015 using high-flow-through passive sampling, Environ. Sci. Technol. 51 (23) (2017) 13929–13937, https://doi.org/10.1021/acs.est.7b04224.
[30] A.P. Francisco, T. Harner, A. Eng, Measurement of polyurethane foam - air partition coefficients for semi-volatile organic compounds as a function of temperature: application to passive air sampler monitoring, Chemosphere 174 (2017) 638–642, https://doi.org/10.1016/j.chemosphere.2017.01.135.
[31] L. Melymuk, P. Bohlin-Nizzetto, R. Prokeš, et al., Sampling artifacts in active air sampling of semi-volatile organic contaminants: comparing theoretical and measured artifacts and evaluating implications for monitoring networks, Environ. Pollut. 217 (2016) 97–106, https://doi.org/10.1016/j.envpol.2015.12.015.
[32] C.K. Qu, A.L. Doherty, X.L. Xing, et al., Chapter 20 – polyurethane foam-based passive air samplers in monitoring persistent organic pollutants: theory and application, in: Environmental Geochemistry, second ed., 2018, pp. 521–542, https://doi.org/10.1016/B978-0-444-63763-5.00021-5.
[33] T.F. Bidleman, O. Nygren, M. Tysklind, Field estimates of polyurethane foam-air partition coefficients for hexachlorobenzene, alpha-hexachlorocyclohexane and bromoanisoles, Chemosphere 159 (2016) 126–131, https://doi.org/10.1016/j.chemosphere.2016.05.040.
[34] Q.L. Cai, X.R. Dai, J.R. Li, et al., The characteristics and mixing states of $PM_{2.5}$ during a winter dust storm in Ningbo of the Yangtze River Delta, China, Sci. Total Environ. 709 (2020) 136146, https://doi.org/10.1016/j.scitotenv.2019.136146.
[35] J.J. Zhang, L. Tong, Z.W. Huang, et al., Seasonal variation and size distributions of water-soluble inorganic ions and carbonaceous aerosols at a coastal site in Ningbo, China, Sci. Total Environ. 639 (2018) 793–803, https://doi.org/10.1016/j.scitotenv.2018.05.183.
[36] M. Mandalakis, A. Besis, E.G. Stephanou, Particle-size distribution and gas/particle partitioning of atmospheric polybrominated diphenyl ethers in urban areas of Greece, Environ. Pollut. 157 (4) (2009) 1227–1233, https://doi.org/10.1016/j.envpol.2008.12.010.
[37] P. Lövkvist, J.A. Jönsson, Capacity of sampling and preconcentration columns with a low number of theoretical plates, Anal. Chem. 59 (6) (1987) 818–821, https://doi.org/10.1021/ac00133a006.
[38] T.F. Bidleman, C.G. Simon, N.F. Burdick, et al., Theoretical plate measurements and collection efficiencies for high-volume air samplers using polyurethane foam, J. Chromatogr. A 301 (1984) 448–453, https://doi.org/10.1016/S0021-9673(01)89218-9, 01.
[39] F. You, T.F. Bidleman, Influence of volatility on the collection of polycyclic aromatic hydrocarbon PAH vapors with polyurethane foam, Environ. Sci. Technol. 18 (5) (1984) 330–333, https://doi.org/10.1021/es00123a008.
[40] Z.W. Huang, C.Y. Huang, C.H. Peng, et al., Penetration behavior of atmospheric polycyclic aromatic hydrocarbons in flow sampler, Environ. Pollut. Control (CN) 39 (11) (2017) 1193–1199, https://doi.org/10.15985/j.cnki.1001-3865.2017.11.007.
[41] T.F. Bidleman, W.N. Billings, W.T. Foreman, Vapor-particle partitioning of semi-volatile organic compounds: estimates from field collections, Environ. Sci. Technol. 20 (10) (1986) 1038–1043, https://doi.org/10.1021/es00152a013.
[42] T.F. Bidleman, A. Leone, Soil-air relationships for toxaphene in the southern United States, Environ. Toxicol. Chem. 23 (10) (2010) 2337–2342, https://doi.org/10.1897/03-405.
[43] W.E. Cotham, T.F. Bidleman, Polycyclic aromatic hydrocarbons and polychlorinated biphenyls in air at an urban and a rural site near lake Michigan, Environ. Sci. Technol. 29 (11) (1995) 2782, https://doi.org/10.1021/es00011a013.
[44] A. Finizio, D. Mackay, T. Bidleman, et al., Octanol-air partition coefficient as a predictor of partitioning of semi-volatile organic chemicals to aerosols, Atmos. Environ. 31 (15) (1997) 2289–2296, https://doi.org/10.1016/S1352-2310(97)00013-7.
[45] F. Wong, P. Kurt-Karakus, T.F. Bidleman, Fate of brominated flame retardants and organochlorine pesticides in urban soil: volatility and degradation, Environ. Sci. Technol. 46 (5) (2012) 2668–2674, https://doi.org/10.1021/es203287x.
[46] J.F. Pankow, Overview of the gas phase retention volume behavior of organic compounds on polyurethane foam, Atmos. Environ. 23 (5) (1989) 1107–1111, https://doi.org/10.1016/0004-6981(89)90311-9.
[47] R.L. Falconer, T.F. Bidleman, Vapor pressures and predicted particle/gas distributions of polychlorinated biphenyl congeners as functions of temperature and ortho-chlorine substitution, Atmos. Environ. 28 (3) (1994) 547–554, https://doi.org/10.1016/1352-2310(94)90130-9.
[48] D. Mackay, W.Y. Shiu, K.C. Ma, et al., Handbook of Physical-Chemical Properties and Environmental Fate for Organic Chemicals, second ed., CRC Press, eBook, 2006 https://doi.org/10.1201/9781420044393. ISBN: 9780429150074.
[49] M. Odabasi, E. Cetin, A. Sofuoglu, Determination of octanol–air partition coefficients and supercooled liquid vapor pressures of PAHs as a function of temperature: application to gas – particle partitioning in an urban atmosphere, Atmos. Environ. 40 (34) (2006) 6615–6625, https://doi.org/10.1016/j.atmosenv.2006.05.051.
[50] H. Xiao, F. Wania, Is vapor pressure or the octanol-air partition coefficient a better descriptor of partitioning between gas phase and organic matter, Atmos. Environ. 37 (20) (2003) 2867–2878, https://doi.org/10.1016/S1352-2310(03)00213-9.
[51] E.O. Gaga, A. Arı, Gas-particle partitioning and health risk estimation of polycyclic aromatic hydrocarbons (PAHs) at urban, suburban and tunnel atmospheres: use of measured EC and OC in model calculations, Atmos. Pollut. Res. 10 (2019) 1–11, https://doi.org/10.1016/j.apr.2018.05.004.
[52] N. Zhang, Y. Yang, Y. Liu, et al., Determination of octanol-air partition coefficients and supercooled liquid vapor pressures of organochlorine pesticides, J. Environ. Sci. Health B 44 (7) (2009) 649–656, https://doi.org/10.1080/03601230903163590.
[53] S. Mahiba, T. Harner, M. Ikonomou, et al., Indoor and outdoor air concentrations and phase partitioning of perfluoroalkyl sulfonamides and polybrominated diphenyl ethers, Environ. Sci. Technol. 38 (5) (2004) 1313–1320, https://doi.org/10.1021/es0305555.
[54] J.F. Pankow, T.F. Bidleman, Interdependence of the slopes and intercepts from log-log correlations of measured gas-particle partitioning and vapor pressure - I. theory and analysis of available data, Atmos. Environ. A. General Topics 26 (6) (1992) 1071–1080, https://doi.org/10.1016/0960-1686(92)90039-N.
[55] K.U. Goss, R.P. Schwarzenbach, Linear free energy relationships used to evaluate equilibrium partitioning of organic compounds, Environ. Sci. Technol. 35 (1) (2001) 1–9, https://doi.org/10.1021/es000996d.
[56] S.C. Grant, V. Schacht, B.I. Escher, et al., Experimental solubility approach to determine PDMS-water partition constants and PDMS activity coefficients, Environ. Sci. Technol. 50 (6) (2016) 3047–3054, https://doi.org/10.1021/acs.est.5b04655.
[57] P. Saranjampour, K. Armbrust, Repeatability of n-octanol/water partition coefficient values between liquid chromatography measurement methods, Environ. Sci. Pollut. Res. 25 (15) (2018) 15111–15119, https://doi.org/10.1007/s11356-018-1729-4.
[58] A.H. Hassan, On the Prediction of Partition Coefficients Using the Statistical Associating Fluid Theory Underpinned by Quantum Mechanical Calculations, Imperial College London, 2016. Doctoral Thesis.
[59] H. Xiao, F. Wania, Evaluation of three prediction methods for partitioning coefficients of organic solutes between a long-chain aliphatic alcohol and the gas phase as a function of temperature, J. Chem. Eng. Data 51 (2) (2006) 330–337, https://doi.org/10.1021/je050369+.
[60] P. Verma, R.D.S. Yadava, Polymer selection for SAW sensor array based electronic noses by fuzzy c -means clustering of partition coefficients: model studies on detection of freshness and spoilage of milk and fish, Sensor. Actuator. B Chem. 209 (2015) 751–769, https://doi.org/10.1016/j.snb.2014.11.149.
[61] N. Ulrich, S. Endo, T.N. Brown, et al., UFZ-LSER Database V 3.2.1 [Internet], Helmholtz Centre for Environmental Research-UFZ, Leipzig, Germany, 2017. Available from: http://www.ufz.de/lser. (Accessed 19 April 2023).